Mon. Not. R. Astron. Soc. **368,** 563–570 (2006) doi:10.1111/j.1365-2966.2006.10116.x

Globular clusters, satellite galaxies and stellar haloes from early dark matter peaks

Ben Moore,[1⋆] Juerg Diemand,[2] Piero Madau,[2] Marcel Zemp[1,3] and Joachim Stadel[1]

[1]*Institute for Theoretical Physics, University of Zürich,CH-8057 Zürich, Switzerland*
[2]*Department of Astronomy and Astrophysics, University of California, Santa Cruz, CA 95064, USA*
[3]*Institute of Astronomy, ETH Zürich, ETH Honggerberg HPF D6, CH-8093 Zürich, Switzerland*

Accepted 2006 January 27. Received 2006 January 22; in original form 2005 October 16

ABSTRACT

The Milky Way contains several distinct old stellar components that provide a fossil record of its formation. We can understand their spatial distribution and kinematics in a hierarchical formation scenario by associating the protogalactic fragments envisaged by Searle & Zinn (1978) with the rare peaks able to cool gas in the cold dark matter density field collapsing at redshift $z > 10$. We use hierarchical structure formation simulations to explore the kinematics and spatial distribution of these early star-forming structures in galaxy haloes today. Most of the protogalaxies rapidly merge, their stellar contents and dark matter becoming smoothly distributed and forming the inner Galactic halo. The metal-poor globular clusters and old halo stars become tracers of this early evolutionary phase, centrally biased and naturally reproducing the observed steep fall off with radius. The most outlying peaks fall in late and survive to the present day as satellite galaxies. The observed radial velocity dispersion profile and the local radial velocity anisotropy of Milky Way halo stars are successfully reproduced in this model. If this epoch of structure formation coincides with a suppression of further cooling into lower sigma peaks then we can reproduce the rarity, kinematics and spatial distribution of satellite galaxies as suggested by Bullock, Kravtsov & Weinberg (2000). Reionization at $z = 12 \pm 2$ provides a natural solution to the missing satellites problem. Measuring the distribution of globular clusters and halo light on scales from galaxies to clusters could be used to constrain global versus local reionization models. If reionization occurs contemporary, our model predicts a constant frequency of blue globulars relative to the host halo mass, except for dwarf galaxies where the average relative frequencies become smaller.

Key words: methods: *N*-body simulations – methods: numerical – galaxies: clusters: general – galaxies: haloes – dark matter.

1 INTRODUCTION

The Milky Way is a typical bright spiral galaxy. Its disc of stars and gas are surrounded by an extended halo of old stars, globular star clusters and a few dark matter dominated old satellite galaxies. For the past 30 yr, two competing scenarios for the origin of galaxies and their stellar components have driven much observational and theoretical research. Eggen, Lynden-Bell & Sandage (1962) proposed a monolithic collapse of the Galaxy whilst Searle & Zinn (1978) advocated accretion of numerous protogalactic fragments.

Enormous progress has been made in understanding the structure and origin of the Milky Way, as well as defining a standard cosmological model for structure formation that provides us with a framework within which to understand our origins (Peebles 1982; Freeman & Bland-Hawthorn 2002). Hierarchical growth of galaxies is a key expectation within a Universe whose mass is dominated by a dark and nearly cold particle [cold dark matter (CDM)], yet evidence for an evolving hierarchy of merging events can be hard to find, since much of this activity took place over 10 billion years ago. The origin of the luminous Galaxy depends on the complex assembly of its $\sim 10^{12}\,M_\odot$ dark halo that extends beyond 200 kpc, and on how stars form within the first dark matter structures massive enough to cool gas to high densities (White & Rees 1978).

The Galactic halo contains about 100 old metal-poor globular clusters (i.e. Forbes et al. 2000), each containing up to 10^6 stars. Their spatial distribution falls off as $r^{-3.5}$ at large radii and half the globulars lie within 5 kpc from the centre of the Galaxy (Strader, Brodie & Forbes 2004). There is no evidence for dark matter within the globular clusters today (Peebles 1984; Moore 1996). The old

⋆E-mail: moore@physik.unizh.ch

stellar halo population has a similar spatial distribution and a total luminosity of 10^8–10^9 $L_\odot$ (Ivezic et al. 2000; Majewski et al. 2000). The stellar populations, ages and metallicities of these components are very similar (Freeman & Bland-Hawthorn 2002).

Also orbiting the Galaxy are several tiny spheroidal satellite galaxies, each containing an old population of stars, some showing evidence for more recent star formation indicating that they can hold on to gas for a Hubble time (Gallagher & Wyse 1994; Grebel, Gallagher & Harbeck 2003). Half of the dwarf satellites lie within 85 kpc, have luminosities in the range 10^6–10^8 $L_\odot$ and are surrounded by dark haloes at least 50–200 times as massive as their baryonic components (Mateo 1998). CDM models have had a notoriously hard time at reconciling the observed low number of satellites with the predicted steep mass function of dark haloes (Kauffmann, White & Guiderdoni 1993; Klypin et al. 1999; Moore et al. 1999).

We wish to explore the hypothesis that CDM dominates structure formation, the haloes of galaxies and clusters are assembled via the hierarchical merging and accretion of smaller progenitors (e.g. Lacey & Cole 1993). This process violently causes structures to come to a new equilibrium by redistributing energy among the collisionless mass components. Early stars formed in these progenitors behave as a collisionless system just like the dark matter particles in their host haloes, and they undergo the same dynamical processes during subsequent mergers and the build-up of larger systems like massive galaxies or clusters.

In a recent study, Diemand, Madau & Moore (2005) used cosmological N-body simulations to explore the distribution and kinematics in present-day CDM haloes of dark matter particles that originally belonged to rare peaks in the matter density field. These properties are particularly relevant for the baryonic tracers of early CDM structures, for example, the old stellar halo which may have originated from the early disruption of numerous dwarf protogalaxies (Bullock et al. 2000), the old halo globular clusters and also giant ellipticals (Gao et al. 2004).

Since rare, early haloes are strongly biased towards overdense regions (e.g. Sheth & Tormen 1999), that is, towards the centres of larger scale fluctuations that have not collapsed yet, we might expect that the contribution at $z = 0$ from the earliest branches of the merger tree is much more centrally concentrated than the overall halo. Indeed, a 'non-linear' peaks biasing has been discussed by previous authors (Moore et al. 1998; White & Springel 2000; Moore 2001). Diemand et al. (2005) showed that the present-day distribution and kinematics of material depend primarily on the rareness of the peaks of the primordial density fluctuation field that the selected matter originally belonged to, that is, when selecting rare density peaks above $\nu\sigma(M, z)$ [where $\sigma(M, z)$ is the linear theory rms density fluctuations smoothed with a top-hat filter of mass M at redshift z], their properties today depend on ν and not on the specific values of selection redshift z and minimal mass M.

In the following section of this paper, we discuss a model for the combined evolution of the dark and old stellar components of the Galaxy within the framework of the Λcold dark matter (ΛCDM) hierarchical model (Peebles 1982). Many previous studies have motivated and touched upon aspects of this work but a single formation scenario for the above components has not been explored in detail and compared with data (Kauffmann, White & Guiderdoni 1993; Bullock, Kravtsov & Weinberg 2000; Côté et al. 2000; Moore 2001; Freeman & Bland-Hawthorn 2002; Benson et al. 2002; Côté, West & Marzke 2002; Somerville, Bullock & Livio 2003; Kravtsov, Gnedin & Klypin 2004; Kravtsov & Gnedin 2005). We assume protogalaxies and globular clusters form within the first rare peaks above a critical mass threshold that can allow gas to cool and form stars in significant numbers (typically at $z \approx 12$). We assume that shortly after the formation of these first systems, the universe reionizes, perhaps by these first protogalaxies, suppressing further formation of cosmic structure until later epochs. We use the N-body simulations to trace the rare peaks to $z = 0$. Most of these protogalaxies and their globular clusters merge together to create the central galactic region. In Section 3, we will compare the spatial distribution and orbital kinematics of these tracer particles with the Galactic halo light and old metal-poor globular clusters. We will see that a small number of these first stellar systems survive as dark matter dominated galaxies. We will compare their properties with the old satellites of the Galaxy in Section 4.

2 THE FIRST STELLAR SYSTEMS

We propose that 'ordinary' Population II stars and globular clusters first appeared in significant numbers at $z > 12$, as the gas within protogalactic haloes with virial temperatures above 10^4 K (corresponding to masses comparable to those of present-day dwarf spheroidals) cooled rapidly due to atomic processes and fragmented. It is this 'second generation' of subgalactic stellar systems, aided perhaps by an earlier generation of metal-free (Population III) stars and by their remnant black holes, which generated enough ultraviolet (UV) radiation to reheat and reionize most of the hydrogen in the Universe by a redshift $z = 12$, thus preventing further accretion of gas into the shallow potential wells that collapsed later. The impact of a high-redshift UV background on structure formation has been invoked by several authors (Haardt & Madau 1996; Bullock et al. 2000; Moore 2001; Barkana & Loeb 2001; Benson et al. 2002; Tully et al. 2002) to explain the flattening of the faint end of the luminosity function and the missing satellites problem within our Local Group. Here, we use high-resolution numerical simulations that follow the full non-linear hierarchical growth of galaxy mass haloes to explore the consequences and predictions of this scenario.

Dark matter structures will collapse at different times, depending on their mass, but also on the underlying larger scale fluctuations. At any epoch, the distribution of masses of collapsed haloes is a steep power law towards low masses with $n(m) \propto \mathrm{m}^{-2}$. To make quantitative predictions, we calculate the non-linear evolution of the matter distribution within a large region of a ΛCDM Universe. The entire well-resolved region is about 10 comoving Mpc across and contains 61 million dark matter particles of mass 5.85×10^5 $M_\odot$ and force resolution of 0.27 kpc. This region is embedded within a larger 90-Mpc cube that is simulated at lower resolution such that the large-scale tidal field is represented. Fig. 1 shows the high-redshift and present-day mass distribution of a single galaxy mass halo taken from this large volume. The rare peaks collapsing at high redshift that have had sufficient time to cool gas and form stars, can be identified, followed and traced to the present day. Because small fluctuations are embedded within a globally larger perturbation, the small rarer peaks that collapse first are closer to the centre of the final potential and they preserve their locality in the present-day galaxy. The strong correlation between initial and final position results in a system where the oldest and rarest peaks are spatially more concentrated than less rare peaks. The present-day spatial clustering of the material that was in collapsed structures at a higher redshift only depends on the rarity of these peaks (Diemand et al. 2005).

Our simulation contains several well-resolved galactic mass haloes which we use to trace the evolution of progenitor haloes that collapse at different epochs. The first metal free Population III stars form within minihaloes already collapsed by $z > 25$, where gas can cool via roto-vibrational levels of H_2 and contract. Their evolution

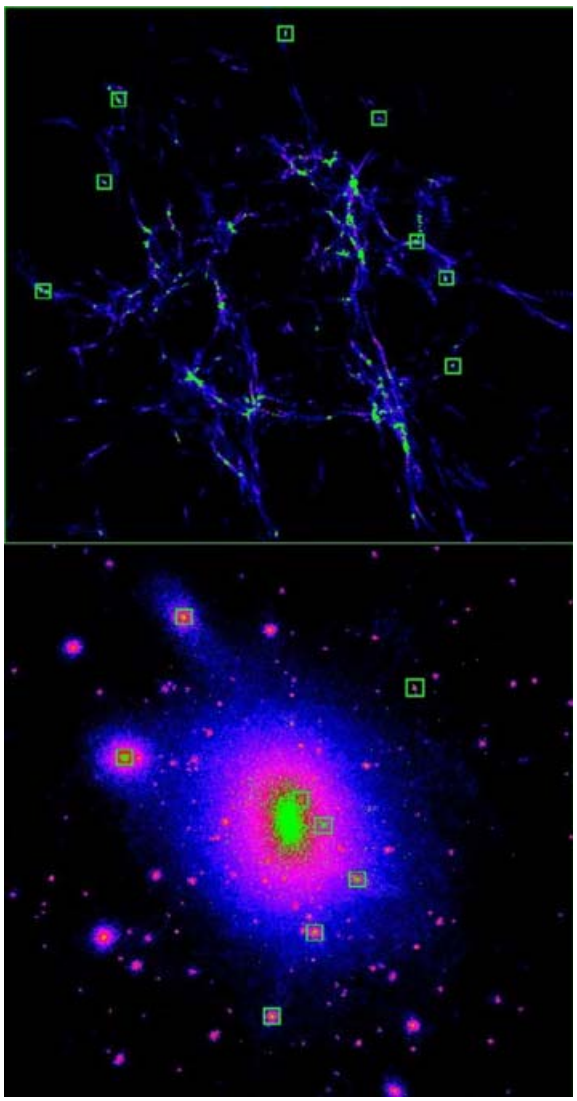

Figure 1. The high-redshift and present-day mass distribution in a region that forms a single galaxy in a hierarchical CDM Universe. The upper panel shows the density distribution at a redshift $z = 12$ from a region that will form a single galaxy at $z = 0$ (lower panel). The blue–pink colour scale shows the density of dark matter whilst the green regions show the particles from protogalaxies with virial temperature above 10^4 K that have collapsed at this epoch. These peaks have masses in the range 10^8–10^{10} $M_\odot$. The lower panel shows same mass distribution at $z = 0$. Most of the rare peaks are located towards the centre of the galaxy today. The squares in both panels indicate those first objects that survive the merging process and can be associated with the visible satellite galaxies today orbiting within the final galactic mass halo. Most of the subhaloes stay dark since they collapse later after reionization has increased the Jeans mass.

is rapid and local metal enrichment occurs from stellar evolution. Metal-poor Population II stars form in large numbers in haloes above $M_H \approx 10^8\,[(1+z)/10]^{-3/2}\,M_\odot$ (virial temperature 10^4 K), where gas can cool efficiently and fragment via excitation of hydrogen Lyα. At $z > 12$, these correspond to $>2.5\sigma$ peaks of the initial Gaussian overdensity field: most of this material ends up within the inner few kpc of the Galaxy. Within the $\approx$1 Mpc turn-around region, a few hundred such protogalaxies are assembling their stellar systems (Kravtsov & Gnedin 2005). Typically 95 per cent of these first structures merge together within a time-scale of a few Gyr, creating the inner Galactic dark halo and its associated old stellar population.

With an efficiency of turning baryons into stars and globular clusters of the order of $f_* = 10$ per cent, we successfully reproduce the total luminosity of the old halo population and the old dwarf spheroidal satellites. The fraction of baryons in dark matter haloes above the atomic cooling mass at $z = 12$ exceeds $f_c = 1$ per cent. A normal stellar population with a Salpeter-type initial mass function emits about 4000 hydrogen-ionizing photons per stellar baryon. A star formation efficiency of 10 per cent therefore implies the emission of $4\,000 \times f_* \times f_c \sim$ a few Lyman-continuum photons per baryon in the Universe. This may be enough to photoionize and drive to a higher adiabatic vast portion of the intergalactic medium, thereby quenching gas accretion and star formation in nearby low-mass haloes.

3 CONNECTION TO GLOBULAR CLUSTERS AND HALO STARS

The globular clusters that were once within the merging protogalaxies are so dense that they survive intact and will orbit freely within the Galaxy. The surviving protogalaxies may be the precursors of the old satellite galaxies, some of which host old globular clusters such as Fornax, whose morphology and stellar populations are determined by ongoing gravitational and hydrodynamical interactions with the Milky Way (e.g. Mayer et al. 2005).

Recent papers have attempted to address the origin of the spatial distribution of globular clusters (e.g. Parmentier & Grebel 2005; Parmentier & Gilmore 2005). Most compelling for this model and one of the key results in this paper is that we naturally reproduce the spatial clustering of each of these old components of the galaxy. The radial distribution of material that formed from $>2.5\sigma$ peaks at $z > 12$ now falls off as $\rho(r) \propto r^{-3.5}$ within the Galactic halo – just as the observed old halo stars and metal-poor globular clusters (cf. Fig. 2).

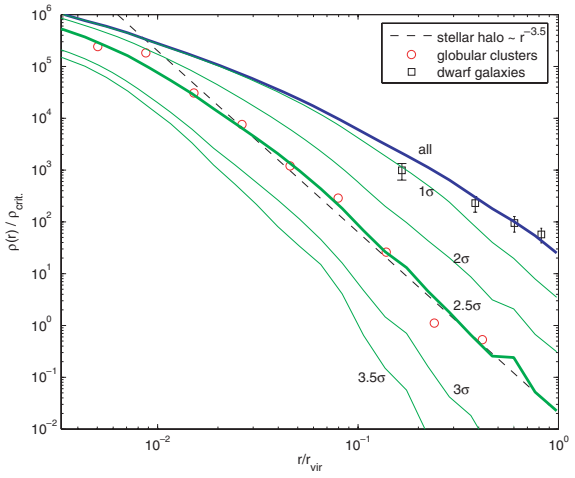

Figure 2. The radial distribution of old stellar systems compared with rare peaks within a $z = 0$ ΛCDM galaxy. The thick blue curve is the total mass distribution today. The labelled green curves show the present-day distribution of material that collapsed into 1, 2, 2.5, 3 and 3.5σ peaks at a redshift $z = 12$. The circles show the observed spatial distribution of the Milky Way's old metal-poor globular cluster system. The dashed line indicates a power law $\rho(r) \propto r^{-3.5}$ which represents the old halo stellar population. The squares show the radial distribution of surviving 2.5σ peaks which are slightly more extended than the overall Navarro–Frenk–White-like mass distribution, in good agreement with the observed spatial distribution of the Milky Way's satellites.

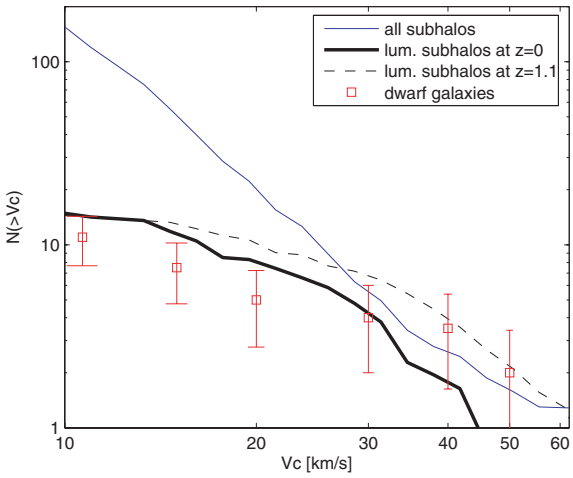

Figure 3. The cumulative velocity distribution function of observed Local Group satellites and predicted dark matter substructures. The red squares show the observed distribution of circular velocities for the Local Group satellites. CDM models predict over an order of magnitude more dark matter substructures than those are observed within the Galactic halo (blue curve). The black solid curve shows the cumulative velocity distribution of present-day surviving substructure haloes that were the rare $>2.5\sigma$ peaks identified at $z = 12$, before they entered a larger mass halo. The dashed curve shows the same objects but at $z = 1.1$ before they entered a larger system in the hierarchy. Their similarity shows that little dynamical evolution has occurred for these objects.

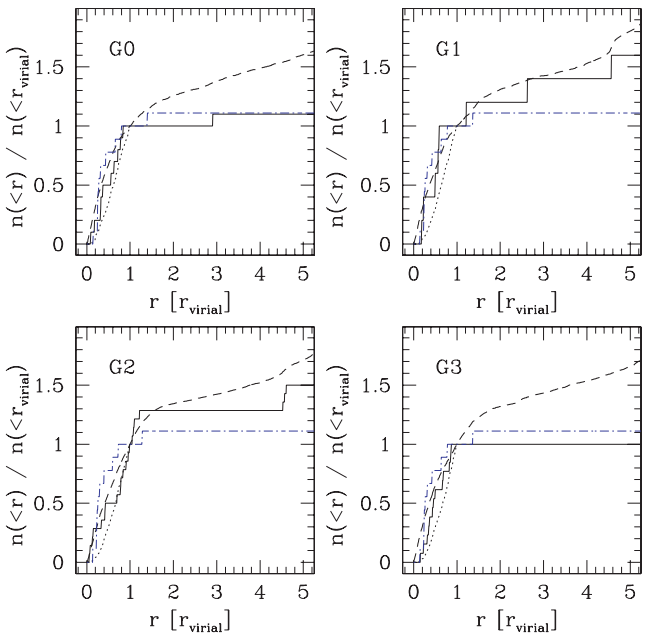

Figure 4. Enclosed number of satellite galaxies (solid lines), all (dark and luminous) subhaloes (dotted) and dark matter particles (dashed) in four CDM galaxy haloes. The numbers are relative to the value within the virial radius. The subhaloes are only plotted out to the viral radius. For comparison with the observed satellite galaxies around the Milky Way (dash–dotted lines) from Mateo (1998) and Wilkinson & Evans (1999), the simulated haloes were rescaled (see Table 1). The satellite galaxy distribution is more concentrated than the one of the total surviving subhalo population but usually more extended than the dark matter particle distribution but there are large differences from one halo to the other. Well beyond the virial radius, the numbers of field dwarf galaxies that will host stars fall below the mean dark matter density.

Cosmological hydrodynamical simulations are also beginning to attain the resolution to resolve the formation of the old stellar haloes of galaxies (Abadi et al. 2006). Because of the steep fall off with radius, we note that we do not expect to find any isolated globular clusters beyond the virial radius of a galaxy.[1]

These first collapsing structures infall radially along filaments and end up significantly more flattened than the mean mass distribution. They also have colder velocity distributions and their orbits are isotropic in the inner halo and increasingly radially anisotropic in the outer part. Material from these rare peaks has $\beta = 1 - (v_t^2/v_r^2) \approx 0.45$ at our position in the Milky Way, in remarkable agreement with the recently measured anisotropy and velocity dispersion of halo stars (Chiba & Beers 2000; Battaglia et al. 2005; Thom et al. 2005). Diemand et al. (2005) show that the radial distribution of rarer peaks is even more highly biased – thus, the oldest Population III stars and their remnant black holes are found mainly within the inner kpc of the Galaxy, falling off with radius steeper than r^{-4}.

The observational evidence for tidal stellar streams from globular clusters suggests that they are not embedded within extended dark matter structures today (Moore 1996). This does not preclude the possibility that the globular clusters formed deep within the central region of $10^8\,M_\odot$ dark haloes which have since merged together. This scenario has been investigated by several authors (Mashchenko & Sills 2004, 2005), who conclude that the kinematics and structural properties of globulars are consistent with a formation history associated with dark matter haloes. (Massive substructure within the inner ~20 per cent $R_{\rm virial}$ of galactic mass haloes is tidally disrupted, i.e. Gihgna et al. 1998.) This is what we expect within our model which would leave the observed globulars freely orbiting without any trace of the original dark matter component. However, it is possible that the most distance halo globulars may still reside within their original dark matter halo. If the globular cluster is located at the centre of the CDM cusp, then observations of their stellar kinematics may reveal rising dispersion profiles. If the globular cluster were orbiting within a CDM minihalo then we would expect to see

[1] The probability to have *one* isolated old globular cluster outside of the virial radius of a Milky Way like galaxy is only 3 per cent in our model.

Table 1. Present-day properties of the four simulated galaxy haloes. The columns give halo name, virial mass, virial radius, peak circular velocity and radius to the peak of the circular velocity curve. The virial radius is defined to enclose a mean density of 98.6 times the critical density. The mass resolution is $5.85 \times 10^5\,M_\odot$ and the force resolution (spline softening length) is 0.27 kpc. For comparison with the Milk Way, these haloes were rescaled to a peak circular velocity of 195 km s^{-1}. In smoothed particle hydrodynamics (SPH) simulations of the same haloes, we found that this rescaling leads to a local rotation speed of 220 km s^{-1} after the baryonic contraction (Maccio' et al. 2006). The rescaled virial radii and virial masses are given in the last two columns.

	$M_{\rm vir}$ ($10^{12}\,M_\odot$)	$r_{\rm vir}$ (kpc)	$V_{\rm c,max}$ (km s^{-1})	$r_{V_{\rm c,max}}$ (kpc)	$M_{\rm MW,vir}$ ($10^{12}\,M_\odot$)	$r_{\rm MW,vir}$ (kpc)
*G*0	1.01	260	160	52.2	1.83	317
*G*1	1.12	268	162	51.3	1.95	323
*G*2	2.21	337	190	94.5	2.39	346
*G*3	1.54	299	180	45.1	1.96	324

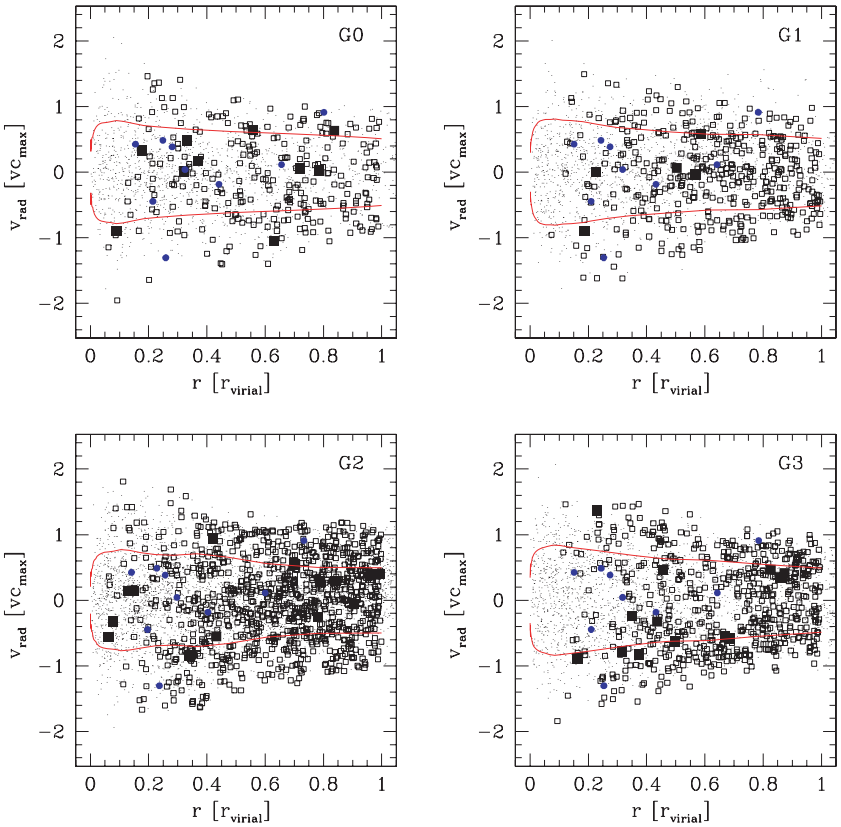

Figure 5. Radial velocities of satellite galaxies (filled squares), all (dark and luminous) subhaloes (open squares) and dark matter particles (small points) in four CDM galaxy haloes. The solid lines are the radial velocity dispersion of the dark matter plotted with positive and negative sign. All quantities are in units of the virial radius and maximum of the circular velocity of the host haloes. For comparison with the observed satellite galaxies around the Milky Way (filled circles) from Mateo (1998) and Wilkinson & Evans (1999), the simulated haloes were rescaled (see Table 1). The observed and the modelled satellite galaxies have similar radial velocities as the dark matter particles while those of the dark subhaloes are larger, especially in the inner part.

symmetric tidal streams orbiting within the potential of the CDM substructure halo rather than being stripped by the Galaxy.

4 CONNECTION TO SATELLITE GALAXIES AND THE MISSING SATELLITES PROBLEM

The remaining ∼5 per cent of the protogalaxies form sufficiently far away from the mayhem that they fall into the assembling galaxy late ($z \approx 1$–2, about 1 Gyr after the formation of the inner Galaxy at $z \approx 5$). This leaves time to enhance their α/Fe element ratios from Type II supernovae (Wyse & Gilmore 1988, 1995; Pritzl, Venn & Irwin 2005). Recent studies including chemical modelling of this process support this scenario (e.g. Font et al. 2006; Robertson et al. 2005).

The protogalaxies highlighted with boxes in Fig. 1 are those few systems that form before reionization and that survive until the present epoch – they all form on the outskirts of the collapsing region, ending up tracing the total mass distribution as is also observed within the Milky Way's and M31's satellite systems. Each of our four high-resolution galaxies contains about 10 of these surviving protogalaxies which have a radial distribution that is slightly *shallower* than that of the total mass distribution but more concentrated than the distribution of all surviving (or $z = 0$ mass selected) subhaloes (Figs 2 and 4). This is consistent with the spatial distribution of surviving satellites in the Milky Way and in other nearby galaxies in the 2dF (Sales & Lambas 2005; van den Bosch et al. 2005) and DEEP2 samples (Coil et al. 2006) and with galaxy groups like NGC 5044 (Faltenbacher & Mathews 2005). [Note that the most massive satellites, such as the Large Magellanic Cloud (LMC) most likely forms more recently, after reionization. Thus, the black curve in Fig. 3 is only relevant for the dwarf spheroidal low-mass satellite population. It should smoothly join the blue curve at 30–40 km s^{-1}.]

Fig. 3 shows the distribution of circular velocities of the Local Group satellites compared with these rare protogalaxies that survive until the present day. The Local Group circular velocity data are the new data from Maccio' et al. (2006), where velocity dispersions have been converted to peak circular velocities using the results of Kazantzidis et al. (2004). The total number of dark matter substructures is over an order of magnitude larger than the observations. Reionization and photoevaporation must play a crucial role in suppressing star formation in less rare peaks, thus keeping most of the low-mass haloes that collapse later devoid of baryons. The surviving population of rare peaks had slightly higher circular velocities just before accretion [at $z \sim 1$, dashed line in Fig. 3 – see Kravtsov et al. (2004)], tidal stripping inside the Galaxy halo then reduced their masses and circular velocities and they match the observations at $z = 0$. Dissipation and tidally induced bar formation could enable satellites to survive even closer to the Galactic Centre (Maccio' et al. 2006).

Likewise to the radial distribution, the kinematics of the *surviving visible* satellite galaxies resembles closely the one of the dark matter while the same properties for all the surviving subhaloes differ

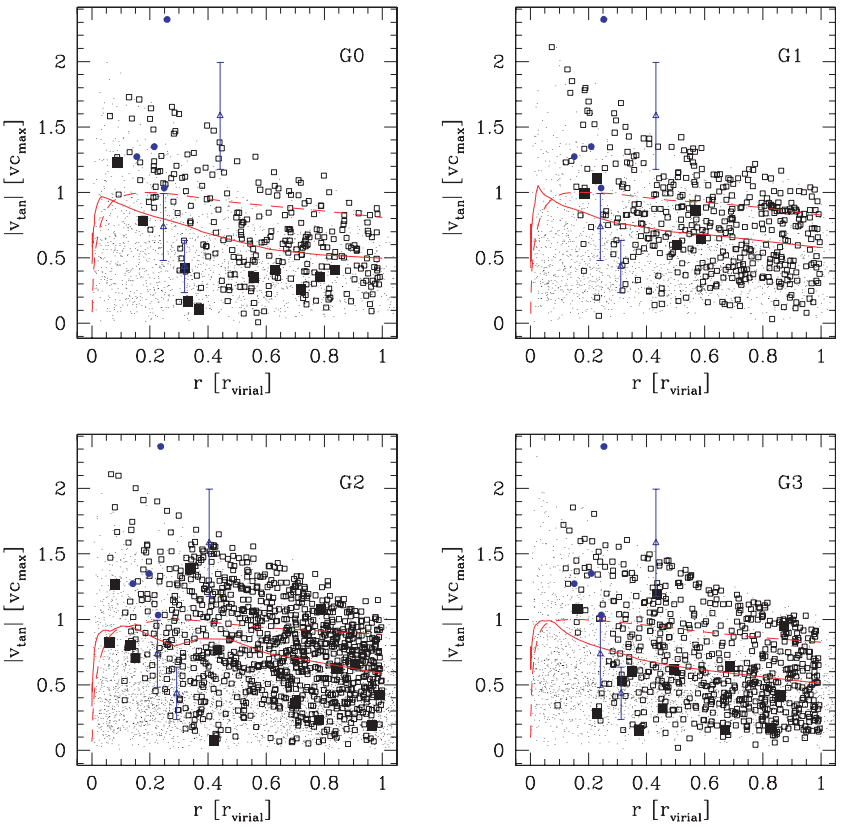

Figure 6. Tangential velocities of satellite galaxies (filled squares), all (dark and luminous) subhaloes (open squares) and dark matter particles (small points) in four CDM galaxy haloes. The lines are the tangential velocity dispersion of the dark matter (solid) and the circular velocity (dashed). The four satellite galaxies (Wilkinson & Evans 1999) give tangential velocities (i.e. from inside out: LMC/Small Magellanic Cloud (SMC), Ursa Minor, Sculptor and Draco) are plotted with filled circles. The open triangles with error bars show *Hubble Space telescope* (*HST*) proper motion data for (from the inside out) Ursa Minor (Piatek et al. 2005), Carina (Piatek et al. 2003) and Fornax (Piatek et al. 2005). The units are as in Fig. 5. The observed and modelled inner satellite galaxies (and also the dark inner subhaloes) have larger typical tangential velocities than the dark matter particles in the same regions.

(Figs 5 and 6). Within the four high-resolution CDM galaxy haloes, our 42 satellite galaxies have average tangential and radial velocity dispersions of $0.70 \pm 0.08 V_{\rm c,max}$ and $0.56 \pm 0.07 V_{\rm c,max}$ respectively, that is, $\beta = 0.26 \pm 0.15$ (the errors are 1σ Poission uncertainties). These values are consistent with those of the dark matter particles: $\sigma_{\rm tan} = 0.66 V_{\rm c,max}$, $\sigma_{\rm rad} = 0.55 V_{\rm c,max}$ and $\beta = 0.30$; the hint of slightly larger dispersions of the satellites are consistent with their somewhat larger radial extent. In the inner part our model, satellite galaxies are hotter than the dark matter background, especially in the tangential component: within $0.3 r_{\rm vir}$, we find $\sigma_{\rm rad,GALS}/\sigma_{\rm rad,DM} = 0.69 V_{\rm cmax}/0.62 V_{\rm c,max} = 1.11$ and $\sigma_{\rm tan,GALS}/\sigma_{\rm tan,DM} = 0.95 V_{\rm c,max}/0.76 V_{\rm c,max} = 1.25$. This is consistent with the observed radial velocities of Milky Way satellites. For the inner satellites, also the tangential motions are known (with large uncertainties however) (e.g. Mateo 1998; Wilkinson & Evans 1999) and just as in our simple model, they are larger than the typical tangential velocities of dark matter particles in the inner halo.

The total (mostly dark) surviving subhalo population is more extended and hotter than the dark matter while the distribution of orbits (i.e. β) is similar (Diemand, Moore & Stadel 2004). For the 2237 subhaloes within the four galaxy haloes, we find $\sigma_{\rm tan} = 0.84 V_{\rm c,max}$, $\sigma_{\rm tan} = 0.67 V_{\rm c,max}$ and $\beta = 0.21$, that is, there is a similar velocity bias relative to the dark matter in both the radial and tangential components and therefore a similar anisotropy. In the inner halo, the differences between dark matter particles and subhaloes are most obvious: within $0.3 r_{\rm vir}$, we find $\sigma_{\rm rad,SUB}/\sigma_{\rm rad,DM} = 0.91 V_{\rm c,max}/0.62 V_{\rm c,max} = 1.47$ and $\sigma_{\rm tan,SUB}/\sigma_{\rm tan,DM} = 1.21 V_{\rm c,max}/0.76 V_{\rm c,max} = 1.59$. Subhaloes tend to avoid the inner halo and those who lie near the centre at $z = 0$ move faster (both in the tangential and radial directions) than the dark matter particles, that is, these inner subhaloes have large orbital energies and spend most of their time further away from the centre (Figs 4–6, see also Diemand et al. 2004).

5 SUMMARY

We have implemented a simple prescription for protogalaxy and globular cluster formation on to a dissipationless CDM N-body simulation. This allows us to trace the kinematics and spatial distribution of these first stellar systems to the final virialized dark matter halo. We can reproduce the basic properties of the Galactic metal-poor globular cluster system, old satellite galaxies and Galactic halo light. More luminous satellites, like the Magellanic Clouds, are in haloes that are massive enough to acquire and cool gas at later times.

The spatial distribution of material within a virialized dark matter structure depends on the rarity of the peak within which the material collapses. This implies a degeneracy between collapse redshift and peak height. For example, 3σ peaks collapsing at $z = 18$ and 10 will have the same final spatial distribution within the Galaxy. However, this degeneracy can be broken since the mass and the numbers of peaks are very different at each redshift. In this example at $z = 18$,

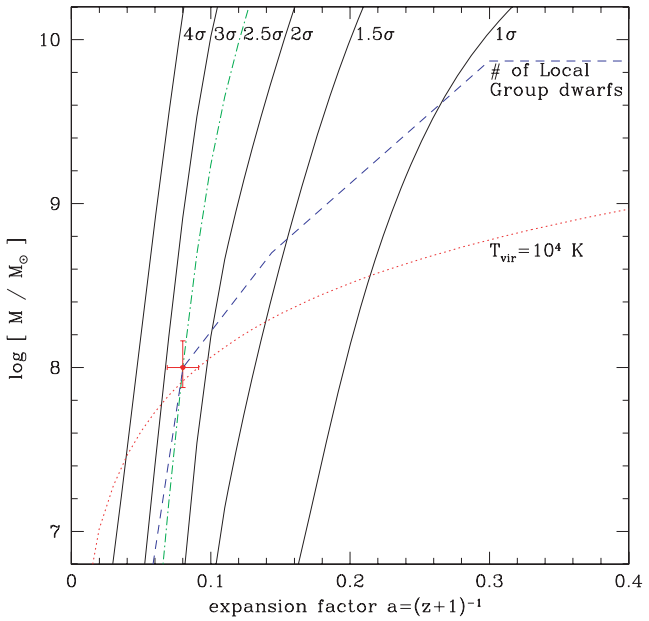

Figure 7. Minimal halo mass for protogalaxy formation versus time. The dashed line connects minimal mass/redshift pairs which produce the number of satellite galaxies observed in the Local Group. If efficient protogalaxy formation is allowed below this line our model would produce too many satellites. The best match to the spatial distribution of globular clusters and stars comes from material that formed within peaks above 2.5σ (dash-dotted lines). The circle with error bars indicates the latest, lowest mass halo which is still allowed to form a protogalaxy. The uncertainty in redshift $z = 11.5^{+2.1}_{-1.5}$ is due to the scatter in our best-fitting redshift when matching the spatial distribution of globular clusters to our individual galaxy halo models at a fixed minimum mass of 10^8 $M_\odot$. The range in minimum masses produces $N_{\rm sat} \pm \sqrt{N_{\rm sat}} \simeq 11 \pm 3$ luminous subhaloes around an average galaxy. The dotted line shows haloes with the atomic cooling virial temperature of 10^4 K. Our inferred minimal mass for efficient protogalaxy formation follows the dotted line until $z = 11.5^{+2.1}_{-1.5}$ and rises steeply (like the 2.5σ line or steeper) after this epoch.

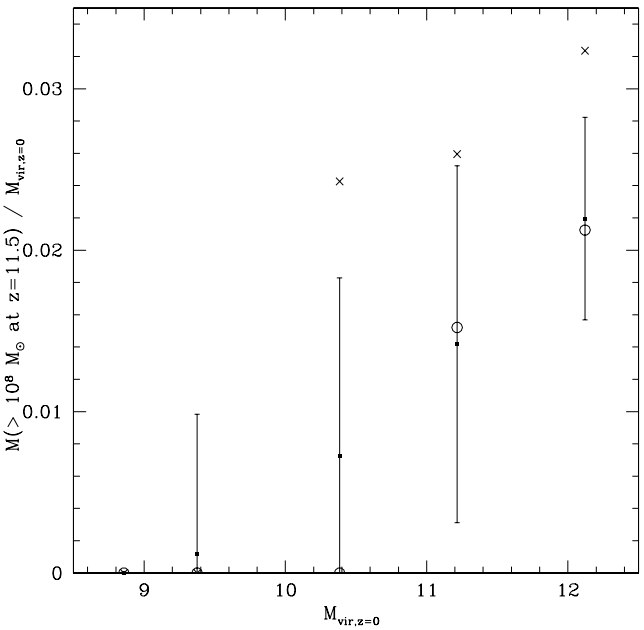

Figure 8. Mass fraction from progenitors which are $>2.5\,\sigma$ peaks for field haloes as a function of their $z = 0$ virial mass. Filled squares with error bars are the mean values and the standard deviations. Median (open circles) 90 percentiles (crosses) of the distributions are also given to illustrate how the shape of the distribution changes for low-mass hosts. In our simple model, this mass fraction is proportional to the mass fraction of Population II stars and metal-poor globular clusters per host halo virial mass. We have no higher mass haloes in the region analysed here but from table 4 in Diemand et al. (2005), we expect constant mass fractions above 10^{12} $M_\odot$.

a galaxy mass perturbation has 700 collapsed 3σ haloes of mass 6×10^6 $M_\odot$, compared to eight peaks of mass 4×10^9 $M_\odot$.

The best match to the spatial distribution of globular clusters and stars comes from material that formed within peaks above 2.5σ. We can then constrain the minimum mass/redshift pair by requiring to match the observed number of satellite galaxies in the Local Group (Fig. 7). If protogalaxies form in early, low-mass 2.5σ peaks, the resulting number of luminous satellites is larger as when they form later in heavier 2.5σ peaks. We find that efficient star formation in haloes above about 10^8 $M_\odot$ up to a redshift $z = 11.5^{+2.1}_{-1.5}$ matches these constraints. The scatter in redshift is due to the different best-fitting redshifts found in our individual galaxy haloes. After this epoch, star formation should be suppressed in small haloes otherwise a too large number of satellites and a too massive and too extended spheroid of Population II stars are produced. The minimum halo mass to form a protogalaxy inferred from these two constraints corresponds to a minimal halo virial temperature of 10^4 K (Fig. 7), that is, just the temperature needed for efficient atomic cooling.

This model is general for galaxy formation, but individual formation histories may reveal more complexity. Soon after reionization, infalling gas into the already massive galactic mass halo leads to the formation of the disc and the metal-enriched population of globular clusters. The first and second generation of stars forming in proto-clusters of galaxies will have a similar formation path, but occurring on a more rapid time-scale.

We find that the mass fraction in peaks of a given σ is independent of the final halo mass, except that it rapidly goes to zero as the host haloes become too small to have sufficiently high σ progenitors [see Fig. 8 and table 4 in Diemand et al. (2005)]. Therefore, if reionization is globally coeval throughout the Universe, the abundance of globulars normalized to the halo mass will be roughly constant in galaxies, groups and clusters. Furthermore, the radial distribution of globular clusters relative to the host halo scale radius will the same (see Diemand et al. 2005). If rarer peaks reionize galaxy clusters earlier (Tully et al. 2002), then their final distribution of blue globulars will fall off more steeply (relative to the scale radius of the host halo) and they will be less abundant per virial mass (Diemand et al. 2005). Observations suggest that the numbers of old globular clusters are correlated with the luminosity of the host galaxy (Harris 1991; McLaughlin 1999; Harris et al. 2006; Rhode, Zepf & Santos 2005). Wide-field surveys of the spatial distribution of globulars in groups and clusters may reveal the details of how and when reionization occurred (Forbes, Brodie & Grillmair 1997; Puzia et al. 2004).

ACKNOWLEDGMENTS

We thank Jean Brodie, Andi Burkert, Duncan Forbes and George Lake for useful discussions and Andrea Maccio' for providing the corrected Local Group data for Fig. 3 prior to publication. All computations were performed on the zBox supercomputer at the University of Zürich. Support for this work was provided by NASA grants

NAG5-11513 and NNG04GK85G, by NSF grant AST-0205738 (PM) and by the Swiss National Science Foundation.

REFERENCES

Abadi M. G., Navarro J. F., Steinmetz M., 2006, MNRAS, 365, 747
Barkana R., Loeb A., 2001, Phys. Rep., 349, 125
Battaglia G. et al., 2005, MNRAS, 364, 433
Benson A. J., Frenk C. S., Lacey C. G., Baugh C. M., Cole S., 2002, MNRAS, 333, 177
Benson A. J., Lacey C. G., Baugh C. M., Cole S., Frenk C. S., 2002, MNRAS, 333, 156
Bland-Hawthorn J., Freeman K., 2000, Sci, 287, 79
Bullock J. S., Kravtsov A. V., Weinberg D. H., 2000, ApJ, 539, 517
Chiba M., Beers T. C., 2000, AJ, 119, 2843
Coil A. L. et al., 2006, ApJ, 638, 668
Cole S., Lacey C., 1996, MNRAS, 281, 716
Côté P., Marzke R. O., West M. J., Minniti D., 2000, ApJ, 533, 869
Côté P., West M. J., Marzke R. O., 2002, ApJ, 567, 853
Diemand J., Moore B., Stadel J., 2004, MNRAS, 352, 535
Diemand J., Madau P., Moore B., 2005, MNRAS, 364, 367
Dubinski J., Carlberg R. G., 1991, ApJ, 378, 496
Eggen O. J., Lynden-Bell D., Sandage A. R., 1962, ApJ, 136, 748
Faltenbacher A., Mathews W. G., 2005, MNRAS, 362, 498
Font A. S., Johnston K. V., Bullock J. S., Robertson B., 2006, ApJ, 638, 650
Forbes D. A., Brodie J. P., Grillmair C. J., 1997, AJ, 113, 1652
Forbes D. A., Masters K. L., Minniti D., Barmby P., 2000, A&A, 358, 471
Freeman K., Bland-Hawthorn J., 2002, ARA&A, 40, 487
Gallagher J. S., Wyse R. F. G., 1994, PASP, 106, 1225
Gao L., Loeb A., Peebles P. J. E., White S. D. M., Jenkins A., 2004, ApJ, 614, 17
Ghigna S., Moore B., Governato F., Lake G., Quinn T., Stadel J., 1998, MNRAS, 300, 146
Grebel E. K., Gallagher J. S., Harbeck D., 2003, AJ, 125, 1926
Haardt F., Madau P., 1996, ApJ, 461, 20
Harris W. E., 1991, ARA&A, 29, 543
Harris W. E., Whitmore B. C., Karakla D., Okon W., Baum W. A., Hanes D. A., Kavelaars J. J., 2006, ApJ, 636, 90
Ivezić Ž. et al., 2000, AJ, 120, 963
Kauffmann G., White S. D. M., Guiderdoni B., 1993, MNRAS, 264, 201
Kazantzidis S., Mayer L., Mastropietro C., Stadel J., Moore B., 2004, ApJ, 608, 663
Klypin A., Kravtsov A. V., Valenzuela O., Prada F., 1999, ApJ, 522, 82
Kravtsov A. V., Gnedin O. Y., Klypin A. A., 2004, ApJ, 609, 482
Kravtsov A. V., Gnedin O. Y., 2005, ApJ, 623, 650
Lacey C., Cole S., 1993, MNRAS, 262, 627
Maccio' A. V., Moore B., Stadel J., Diemand J., 2006, MNRAS, 366, 1529
Mackey A. D., van den Bergh S., 2005, MNRAS, 360, 631
Majewski S. R., Ostheimer J. C., Patterson R. J., Kunkel W. E., Johnston K. V., Geisler D., 2000, AJ, 119, 760
Mashchenko S., Sills A., 2004, ApJ, 605, L121
Mashchenko S., Sills A., 2005, ApJ, 619, 243
Mateo M. L., 1998, ARA&A, 36, 435
Mayer L., Mastropietro C., Wadsley J., Stadel J., Moore B., 2005, MNRAS, submitted (astro-ph/0504277)
McLaughlin D. E., 1999, AJ, 117, 2398
Moore B., 1996, ApJ, 461, L13
Moore B., 2000, AIP Conf. Proc. 586, The Dark Matter Crisis (Plenary Talk). 586, 73
Moore B., Governato F., Quinn T., Stadel J., Lake G., 1998, ApJ, 499, L5
Moore B., Ghigna S., Governato F., Lake G., Quinn T., Stadel J., Tozzi P., 1999, ApJ, 524, L19
Parmentier G., Gilmore G., 2005, MNRAS, 363, 326
Parmentier G., Grebel E. K., 2005, MNRAS, 359, 615
Peebles P. J. E., 1982, ApJ, 263, L1
Peebles P. J. E., 1984, ApJ, 277, 470
Piatek S. et al., 2002, AJ, 124, 3198
Piatek S., Pryor C., Olszewski E. W., Harris H. C., Mateo M., Minniti D., Tinney C. G., 2003, AJ, 126, 2346
Piatek S., Pryor C., Bristow P., Olszewski E. W., Harris H. C., Mateo M., Minniti D., Tinney C. G., 2005, AJ, 130, 95
Pritzl B. J., Venn K. A., Irwin M. J., 2005, AJ, 130, 2140
Puzia T. H. et al., 2004, A&A, 415, 123
Rhode K. L., Zepf S. E., Santos M. R., 2005, ApJ, 630, L21
Robertson B., Bullock J. S., Font A. S., Johnston K. V., Hernquist L., 2005, ApJ, 632, 872
Sales L., Lambas D. G., 2005, MNRAS, 356, 1045
Searle L., Zinn R., 1978, ApJ, 225, 357
Sheth R. K., Tormen G., 1999, MNRAS, 308, 119
Somerville R. S., Bullock J. S., Livio M., 2003, ApJ, 593, 616
Strader J., Brodie J. P., Forbes D. A., 2004, AJ, 127, 3431
Strader J., Brodie J. P., Cenarro A. J., Beasley M. A., Forbes D. A., 2005, AJ, in press.
Thom C. et al., 2005, MNRAS, 360, 354
Tully R. B., Somerville R. S., Trentham N., Verheijen M. A. W., 2002, ApJ, 569, 573
van den Bosch F. C., Yang X., Mo H. J., Norberg P., 2005, MNRAS, 356, 1233
Wilkinson M. I., Evans N. W., 1999, MNRAS, 310, 645
White S. D. M., Rees M. J., 1978, MNRAS, 183, 341
White S. D. M., Springel V., 2000, in Weiss A., Abel T. G., Hill V., eds, The First Stars. Proc. MPA/ESO Workshop. Springer, Berlin, p. 327
Wyse R. F. G., Gilmore G., 1988, AJ, 95, 1404
Wyse R. F. G., Gilmore G., 1995, AJ, 110, 2771

This paper has been typeset from a TEX/LATEX file prepared by the author.